

## Supercollimation in photonic crystals composed of silicon rods

Ta-Ming Shih,<sup>1,a)</sup> André Kurs,<sup>1</sup> Marcus Dahlem,<sup>1</sup> Gale Petrich,<sup>1</sup> Marin Soljačić,<sup>1</sup> Erich Ippen,<sup>1</sup> Leslie Kolodziejski,<sup>1</sup> Katherine Hall,<sup>2</sup> and Morris Kesler<sup>2</sup>

<sup>1</sup>Research Laboratory of Electronics, Massachusetts Institute of Technology, 77 Massachusetts Ave., Cambridge, Massachusetts 02139, USA

<sup>2</sup>Wide Net Technologies, 80 Coolidge Hill Rd., Watertown, Massachusetts 02472, USA

(Received 19 June 2008; accepted 10 September 2008; published online 3 October 2008)

Supercollimation is the propagation of light without diffraction using the properties of photonic crystals. We present the first experimental demonstration of supercollimation in a planar photonic crystal composed of nanoscale rods. Supercollimation was observed over distances of up to 1000 lattice periods. © 2008 American Institute of Physics. [DOI: 10.1063/1.2992198]

Photonic crystals (PhCs) provide an exciting platform for the control of light.<sup>1</sup> The appropriate design of a PhC gives rise to properties that enable supercollimation (SC), the propagation of a light beam without diffraction.<sup>2</sup> In contrast to gap-guided modes due to defects in PhCs, supercollimating modes are propagating eigenmodes of a perfectly periodic PhC. Supercollimators with nanoscale features are capable of providing transmission over distances on the order of centimeters and may potentially find use for integrated optical interconnects.<sup>3,4</sup> SC has been previously demonstrated in planar [two-dimensional slab (2D-slab)] PhCs of air holes in dielectric slabs.<sup>3-5</sup> Beam propagation in an arrayed waveguide structure has been investigated in Ref. 6. We present the first experimental demonstration of SC in a 2D-slab PhC that is composed of dielectric rods.

SC occurs in a PhC whose band structure contains equifrequency contours that have flat sections. As seen in Fig. 1, a single-frequency beam composed of eigenmodes from a flat portion of the contour for  $\lambda=1550$  nm experiences little divergence (no divergence at all if the contour were perfectly flat) as it propagates along the  $\Gamma$ - $M$  direction because the group velocities for all of the beam's constituent eigenmodes point in the  $\Gamma$ - $M$  direction. The free-space wavelength of the flattest contour is referred to as  $\lambda_{sc}$ , and the  $\Gamma$ - $M$  direction is referred to as the SC direction. The band structure for a PhC composed of a square lattice of air holes in a dielectric slab has similar qualitative features.

The supercollimating PhC that was designed and simulated using the MIT PHOTONIC BANDS software package,<sup>7</sup> consists of a square lattice of silicon rods ( $n_{Si}=3.52$  at  $\lambda=1550$  nm) with period  $a=437.5$  nm, rod radius  $r=125$  nm, and rod height  $h=700$  nm. The light is confined in the vertical direction by index guiding, which is achieved by having a 3- $\mu$ m-thick layer of lower index SiO<sub>2</sub> ( $n_{Ox}=1.53$ ) separating the layer of Si rods from the underlying Si substrate. The PhC structure was designed so that  $\lambda_{sc}$  is close to 1550 nm.

Although the equifrequency contours are not perfectly flat, it is possible in principle to create a beam that experiences an arbitrarily flat portion of a contour by making the distribution of the beam's constituent eigenmodes sufficiently narrow in  $k$ -space, i.e., as the beam approaches a

single Bloch mode. However, the supercollimator allows for nearly divergent-less propagation for beam widths only a few times the lattice constant of the PhC. The range of  $k$ -vectors over which a beam is well collimated is referred to as the spatial frequency bandwidth of the supercollimator, which sets the scale for the minimum beam width capable of SC. The range of wavelengths over which a beam is well collimated is referred to as the temporal frequency bandwidth.

The bandwidths in the spatial and temporal frequency domains determine the performance, as well as the fabrication and measurement tolerances of the supercollimator. One method of exploring the design space for supercollimating devices is illustrated by Fig. 2, which shows SC length as a function of initial beam width and wavelength for (i) the PhC of rods and (ii) an analogous PhC of air holes in a dielectric slab.<sup>4</sup> The SC length is defined as the propagation distance over which the width of an initial Gaussian beam increases by a factor of  $\sqrt{2}$ . In general, a Gaussian beam will not remain Gaussian during propagation within a supercollimator. Therefore, the beam width is defined here as the width which encloses  $\text{erf}(\sqrt{2}) \approx 0.9545$  of the total intensity. In the case of free space Gaussian propagation, this definition of beam

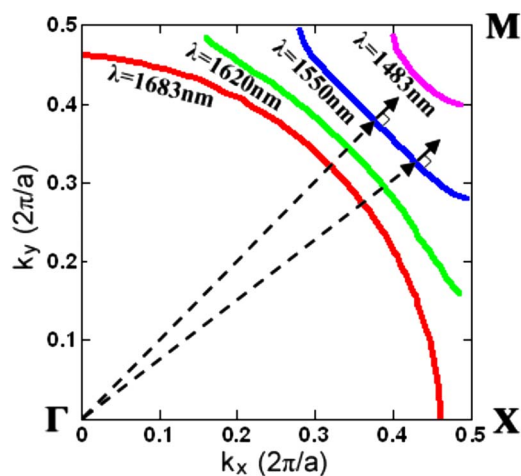


FIG. 1. (Color online) The TM-like equifrequency contours of the first band from a 3D simulation of the designed supercollimating PhC consisting of a square lattice of rods. The dashed arrows indicate the in-plane wave vectors while the solid arrows indicate the group velocities of the corresponding waves inside the PhC. The free-space wavelength of the flattest contour along the  $\Gamma$ - $M$  direction,  $\lambda_{sc}$ , is 1550 nm.

<sup>a)</sup>Electronic mail: shihmt@mit.edu.

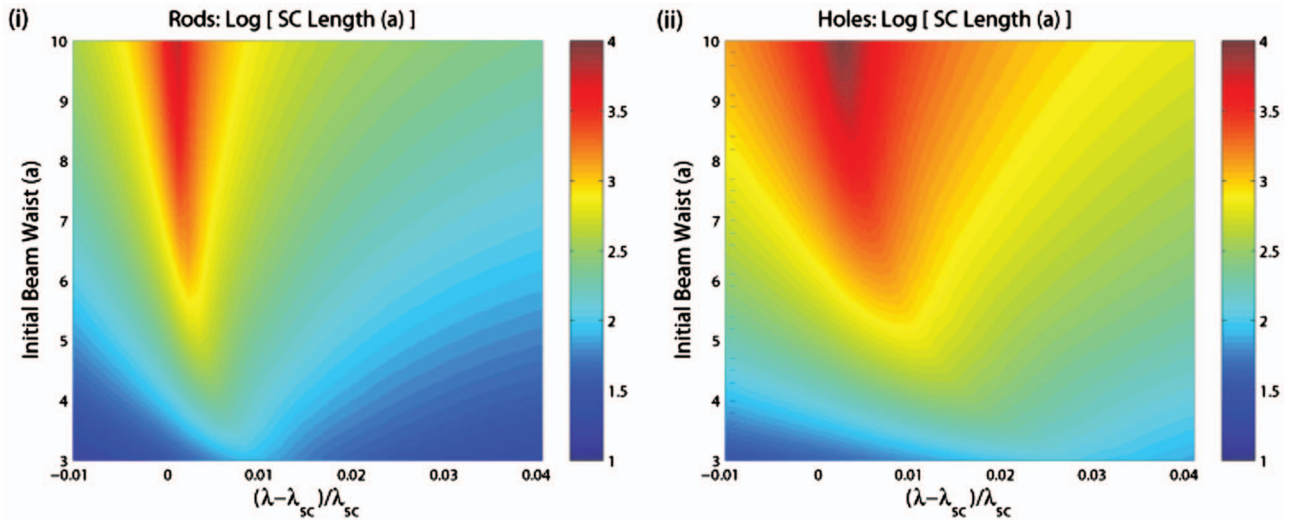


FIG. 2. (Color) The logarithm of the SC length normalized by the periodicity  $a$  as a function of initial beam waist normalized by  $a$  and fractional change in wavelength from  $\lambda_{sc}$ , for a PhC composed of (i) a square lattice of Si rods in air on  $\text{SiO}_2$  (with dimensions  $a=437.5$  nm,  $r=125$  nm, and  $h=700$  nm), for which the supercollimating modes are TM-like, and (ii) a square lattice of air holes in Si on  $\text{SiO}_2$  (with dimensions  $a=350$  nm,  $r=105$  nm, and  $h=205$  nm), for which the supercollimating modes are TE-like.

width reduces to twice the beam waist, and the diffraction length reduces to the usual formula of  $L = \pi w_0^2 / \lambda$ . Assuming an initial Gaussian beam waist profile that is propagating in the  $\Gamma-M$  direction, the beam propagation method was used to calculate the SC length from a fourth-order polynomial fit of the simulated dispersion relation of Fig. 1.

Due to the effect of higher order terms that describe the equifrequency contour, the wavelengths at which the beam is best collimated (longest SC length), given a fixed initial beam width, are longer than  $\lambda_{sc}$ . This is due to the effect of the quartic term, which, for  $\lambda < \lambda_{sc}$ , adds to the curvature caused by the quadratic term, but offsets the effect of the quadratic term for  $\lambda > \lambda_{sc}$ . As the initial beam width is increased, however, the effect of the quadratic term becomes dominant and the optimal wavelength asymptotes to  $\lambda_{sc}$ .

There are notable differences between the SC properties of the PhC of rods and the analogous PhC of air holes in a dielectric slab. Whereas the supercollimating eigenmodes in a lattice of air holes are TE-like (electric field in the plane of the slab), those in a lattice of dielectric rods are TM-like. An analytical perturbative analysis shows that in response to small changes in the dielectric medium surrounding the rods,

the eigenfrequencies of the supercollimating eigenmodes in a lattice of rods shift roughly six times as much as in a lattice of air holes with similar dimensions in a dielectric slab. Note also, from Fig. 2, that the temporal frequency bandwidth over which the beam is well collimated is narrower in the case of the PhC of rods, causing the structure to be more challenging to fabricate and measure.

The PhC of rods was fabricated on a silicon-on-insulator (SOI) substrate having a 700-nm-thick Si layer and a 3- $\mu\text{m}$ -thick buried  $\text{SiO}_2$  layer. Plasma-enhanced chemical vapor deposition (PECVD) was used to deposit an etch mask of 120-nm-thick  $\text{SiO}_2$  on the SOI substrate, which was followed by the application of a trilayer resist stack consisting of antireflective coating, followed by  $\text{SiO}_2$ , and finally followed by photoresist. Large-area pattern definition of the nanoscale rods was achieved with two orthogonal interference lithography exposures, followed by photoresist development. Pattern transfer, from the photoresist through the intermediary layers to the Si layer, was achieved with reactive ion etching (RIE). A sequence of RIE steps using  $\text{CF}_4$  and  $\text{He}/\text{O}_2$  was used to transfer the pattern through the trilayer resist stack. The pattern was then transferred to the PECVD  $\text{SiO}_2$  etch mask by RIE using a  $\text{CF}_4$  plasma. Reactive ion etching with  $\text{Cl}_2$  was used to pattern the rods in the Si device layer. Any remaining  $\text{SiO}_2$  etch mask was not removed, resulting in a more symmetric oxide-silicon-oxide structure. Figure 3 is a scanning electron micrograph (SEM) of a fabricated device, showing the desired nanoscale features. The wafer was cleaved into rectangular samples ranging from 2 to 7 mm on a side.

To demonstrate SC, TM-polarized light from a tunable laser source was coupled into the supercollimator sample through a high-NA single-mode lensed fiber with a  $1/e$  spot size of 2.5  $\mu\text{m}$  at the PhC facet. The light that was scattered out of the plane due to structural imperfections (e.g., sidewall roughness) during propagation was then captured with an infrared camera,<sup>4</sup> producing the images of Fig. 4. The experimentally observed optimal wavelength varied for different samples, ranging from 1530 to 1550 nm. This varia-

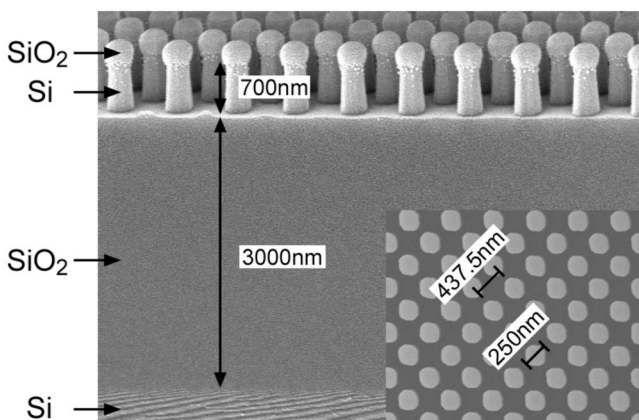


FIG. 3. Side-view SEM of the fabricated large-area supercollimating PhC. Inset: plan-view SEM of the same device.

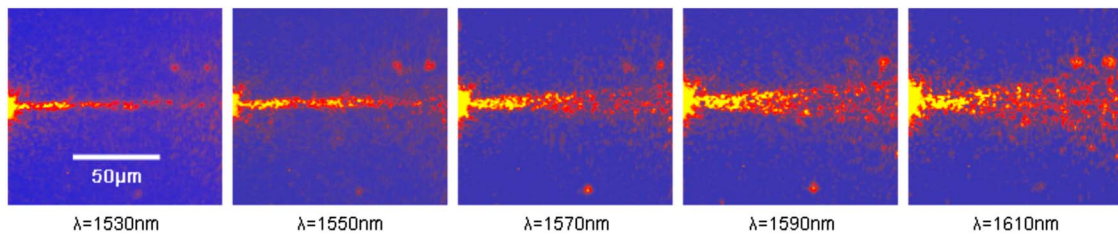


FIG. 4. (Color online) Plan view infrared images on the same scale, with equal  $x$  and  $y$  scaling, showing the wavelength dependence of the propagating beam inside the 2D-slab PhC of rods. The optimal wavelength of SC is close to 1530 nm, and the beam diverges for nonoptimal wavelengths.

tion is due to the nonuniformity of the rod radius across the wafer during fabrication. For wavelengths that are nonoptimal, the beam is observed to exhibit divergent propagation. SC is shown in Fig. 4 for more than 200 lattice periods or about eight isotropic diffraction lengths. An isotropic diffraction length is the distance over which the  $1/e$  width of a Gaussian optical beam increases by a factor of  $\sqrt{2}$  in air. SC distances of up to 1000 lattice periods have also been observed in the laboratory.

In summary, SC at wavelengths ranging from 1530 to 1550 nm has been demonstrated over distances of hundreds of microns in PhCs that are composed of dielectric (Si) rods. In contrast to an analogous supercollimator composed of air holes in a dielectric slab, the supercollimator of rods exhibits a roughly sixfold increase in sensitivity to changes in the ambient medium and a narrower temporal frequency bandwidth. Such differences suggest that air holes are more suitable for communications applications while rods are more suitable for applications such as sensing, since light interacts with the medium (to be sensed) that surrounds the rods six times more strongly. Rod-based PhCs may also find use in optofluidics, where the rod structure may allow for better fluid penetration than air holes in a dielectric slab.

The Si-based material system is well suited for the optoelectronic integration of supercollimating devices.

The authors acknowledge the support of the Interconnect Focus Center, one of five research centers funded under the Focus Center Research Program, a Semiconductor Research Corporation and DARPA program contract No. B-12-M06-52. The authors acknowledge AFOSR Contracts Nos. FA9550-07-C-0005 and FA9550-07-1-0014, the MRSEC program of the NSF under DMR 02-13282, and the Army Research Office through the Institute for Soldier Nanotechnologies under Contract No. W911NF-07-D-0004.

<sup>1</sup>J. Joannopoulos, R. Meade, and J. Winn, *Photonic Crystals: Molding the Flow of Light* (Princeton University Press, Princeton, 1995).

<sup>2</sup>H. Kosaka, T. Kawashima, A. Tomita, M. Notomi, T. Tamamura, T. Sato, and S. Kawakami, *Appl. Phys. Lett.* **74**, 1212 (1999).

<sup>3</sup>D. Prather, S. Shi, J. Murakowski, G. Schneider, A. Sharkawy, C. Chen, B. Miao, and R. Martin, *J. Phys. D: Appl. Phys.* **40**, 2635 (2007).

<sup>4</sup>P. Rakich, M. Dahlem, S. Tandon, M. Ibanescu, M. Soljačić, G. Petrich, J. Joannopoulos, L. Kolodziejski, and E. Ippen, *Nat. Mater.* **5**, 93 (2006).

<sup>5</sup>L. Wu, M. Mazilu, and T. Krauss, *J. Lightwave Technol.* **21**, 561 (2003).

<sup>6</sup>T. Pertsch, T. Zentgraf, U. Peschel, A. Bräuer, and F. Lederer, *Phys. Rev. Lett.* **88**, 093901 (2002).

<sup>7</sup>S. Johnson and J. Joannopoulos, *Opt. Express* **8**, 173 (2001).